THE JOURNAL OF PHYSICAL CHEMISTRY C

Article

Cite This: J. Phys. Chem. C 2020, 124, 799−804

pubs.acs.org/JPCC

Unravelling Reaction Products of Styrene Oxide Adsorbed on Ag(111) Using REMPI-Assisted Temperature-Programmed Desorption

Georg Westphal,[†] Mareike Wallrabe,[†] and Tim Schäfer*[,†,‡]

[†]Institute of Physical Chemistry, Georg-August University of Goettingen, Tammannstraße 6, 37077 Goettingen, Germany

[‡]Max Planck Institute for Biophysical Chemistry, Am Fassberg 11, 37077 Goettingen, Germany

ABSTRACT: Adsorption of styrene oxide on Ag(111) at 200 K leads to the formation of a stable oxametallacycle by ring-opening of the epoxide. At elevated temperatures, the oxametallacycle reacts and the products desorb from the surface. We employ resonance-enhanced multiphoton ionization time-of-flight mass spectrometry (REMPI-ToF-MS) to identify reaction products after desorption. We assign phenylacetaldehyde as the only product that desorbs at temperatures around 485 K.

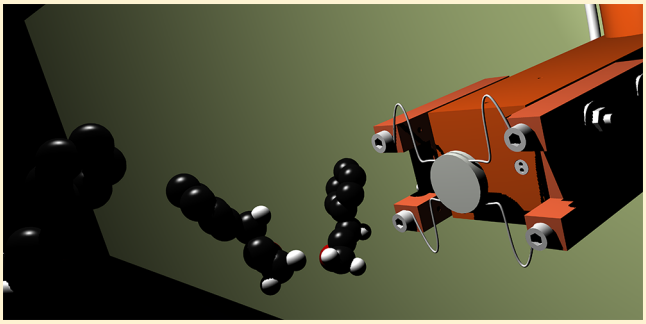

INTRODUCTION

Heterogeneously catalyzed epoxidation of unsaturated hydrocarbons on silver-based catalysts is an important class of chemical reactions with industrial relevance.[1] Strong efforts have been made in the past decades to study the underlying reaction mechanism at the surface by using experimental techniques like temperature-programmed desorption (TPD), X-ray photoelectron spectroscopy (XPS), reflection absorption−infrared spectroscopy (RAIRS), and high-resolution electron energy loss spectroscopy (HREELS) supported by density functional theory (DFT)-based calculations.[2−13] By pursuing the classical surface science approach, which means reducing the real-world catalyst's complexity to a well-defined single-crystal environment under ultrahigh-vacuum conditions, details of the underlying reaction pathways at the surface have been elucidated. The partial oxidation of styrene on an oxidized Ag(111) surface proceeds via an oxametallacycle intermediate, as confirmed experimentally by TPD and XPS studies.[10−12,14,15] The same oxametallacycle is also produced by ring-opening when styrene oxide is dosed onto clean Ag(111), which provides a convenient method for studying its reactivity. For studies on the intermediate oxametallacycle, it is therefore convenient to investigate the styrene oxide/Ag(111) system as done by Enever et al.[16] In a combined TPD, HREELS, and DFT study they observe a prominent peak in the TPD spectrum at elevated temperatures around 485 K, which they assign predominantly to desorption of styrene oxide after reversible ring closure of the oxametallacyle. The assignment of the oxametallacyle is supported by HREELS measurements at surface temperatures below desorption and by DFT calculations. Desorbing styrene oxide was detected by mass spectrometry after electron impact ionization. While this technique is universal and easy to implement, it has limitations in distinguishing molecular isomers. In general, three structural isomers—styrene oxide (**1**), phenylacetaldehyde (**2**), and acetophenone (**3**)—are conceivable reaction products after surface reaction of the oxametallacycle and subsequent desorption (see Scheme 1).

Scheme 1. Adsorption of Styrene Oxide on Ag(111) and Possible Reaction Products after Desorption: Styrene Oxide (1), Phenylacetaldehyde (2), and Acetophenone (3)

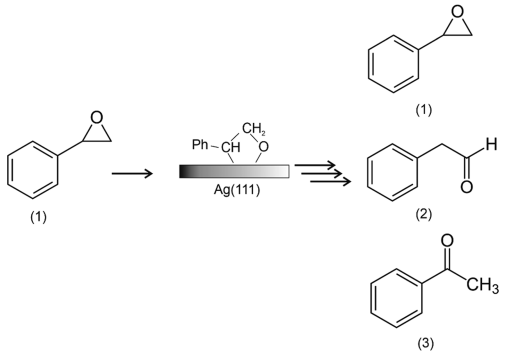

Enever et al. recorded fragmentation patterns after electron impact (EI) ionization of the desorbing molecules and used the different fragmentation patterns of structural isomers for isomer identification. However, this approach is challenging when the fragmentations of different isomers are similar—in particular when the mass spectrum is recorded during a

Received: November 4, 2019
Revised: December 3, 2019
Published: December 4, 2019

DOI: 10.1021/acs.jpcc.9b10358
J. Phys. Chem. C 2020, 124, 799−804

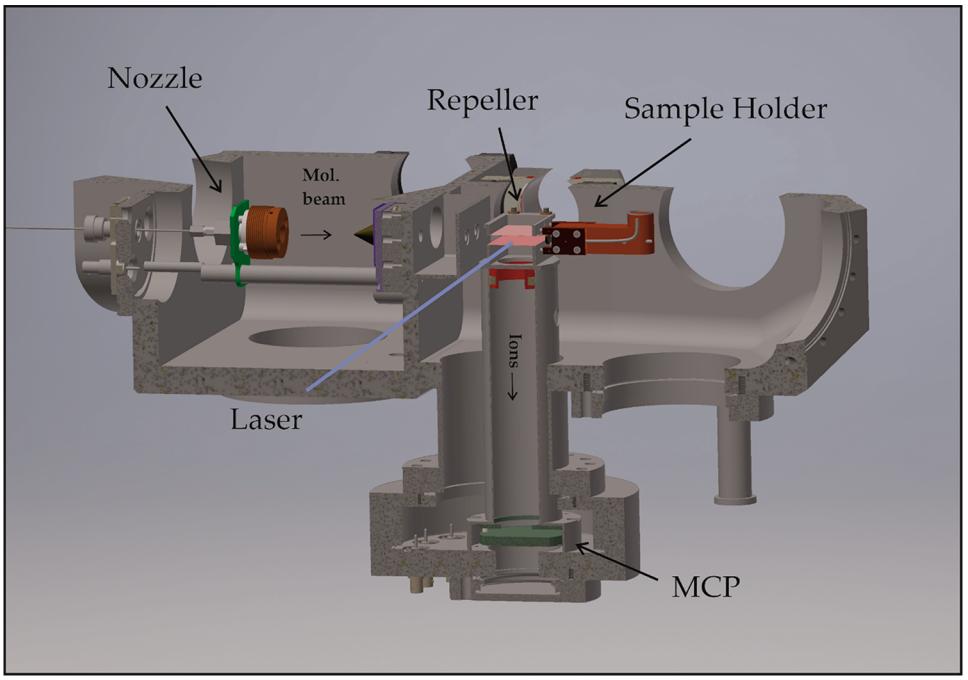

Figure 1. Experimental setup for REMPI-assisted TPD experiments. The apparatus consists of the UHV chamber, source chamber, and differentially pumped chamber. Styrene oxide is dosed onto the surface by a supersonic molecular beam generated by a nozzle that is oriented normal to the surface. The surface is mounted on a sample holder that can be positioned into the molecular beam by a manipulator. After dosing, the surface temperature is linearly ramped by resistive heating. Desorbing molecules fly into the ionization region of the ToF mass spectrometer. Desorbing molecules are ionized by laser radiation, and the ions are coupled into the ToF mass spectrometer by a repeller and extractor, which are designed from grids to avoid local pressure rises.

temperature-programmed desorption scan in which the desorbing molecules are detectable only on a short time scale and might even be overlapped by other reaction products with similar desorption temperature. Furthermore, there are inconsistencies in the literature concerning the ring closure of the oxametallacycle to styrene oxide. For instance, Zhou et al.[10,11] observe a significantly lower desorption temperature for styrene oxide after ring closure in their investigation of the oxidation of styrene on oxidized Ag(111).

In this paper we employ REMPI-assisted temperature-programmed desorption (TPD) on the styrene oxide/Ag(111) system which provides unambiguous isomer identification. We follow the lines recently developed by Sugimoto et al.[17] and Winbauer et al.[18] The surface is dosed with a molecular beam of styrene oxide seeded in argon, and desorbing molecules are detected during a TPD scan using resonance-enhanced multiphoton ionization (REMPI) in combination with time-of-flight (ToF) mass spectrometry. We distinguish isomers by different ionization probabilities. This allows us to assign the high-temperature peak in the TPD spectrum unambiguously to phenylacetaldehyde, in contrast to previous studies.

EXPERIMENTAL SECTION

Experiments have been performed in a UHV surface science chamber depicted in Figure 1. For recording REMPI spectra of possible reaction products, we ionize molecules in a pulsed molecular beam at 10 Hz repetition rate. The molecular beam is produced in a home-built pulsed solenoid nozzle based on the Even-Lavie design and skimmed by a 1.5 mm electro-formed skimmer (Ni Model 2, Beam Dynamics, Inc.). Pure styrene oxide (97% purity), acetophenone (99.5% purity), or phenylacetaldehyde (95% purity) was placed in a sample compartment near the tip of the nozzle and introduced to the molecular beam pulse by gentle resistive heating of the nozzle tip to 350 K, as described in previous work.[19,20] Water was removed by passing the carrier gas through a sample of $MgSO_4$ (99% purity). For the REMPI spectra we use He as carrier gas to avoid clustering. The incidence translational energy was measured by using ion imaging techniques as described in detail in ref 21. Chemicals have been purchased at Sigma-Aldrich and were used without further purification. We use two different REMPI schemes for ionizing the molecules. Styrene oxide, acetophenone, and phenylacetaldehyde have vertical ionization potentials of 9.2,[22] 9.38,[23] and 9.15 eV,[24] respectively. In the first scheme, we ionize via the π^* state by a 1 + 1 REMPI process employing nanosecond laser pulses around 265 nm. UV photons are generated by the second harmonic output (1.5 mJ/pulse) of a Nd:YAG (LabPRO-200, Spectra-Physics, 10 Hz, 12 ns) pumped dye laser (PRSC-DA-24, Sirah). In a second scheme, we ionize via low-lying Rydberg states in a 2 + 1 REMPI process using a femtosecond laser pulse at around 370 nm obtained from the output of an optical parametric amplifier (OPA, Topas Prime+) pumped by the 800 nm output of a Ti:Sa laser equipped with a regenerative amplifier (Solstice, 5 mJ, <35 fs, Spectra-Physics). Ions are detected on microchannel plates (Z-stack), which are capacitatively coupled to an oscilloscope. For 2 + 1 REMPI we focus the laser beam using a convex lens with a focal length of f = 250 mm. We do not focus for 1 + 1 REMPI.

For REMPI-TPD experiments, we employ a molecular beam for dosing a Ag(111) crystal with controlled incidence translational energy and little spatial spread. The Ag(111) crystal is mounted on a sample holder and can be temperature controlled between 110 and 1235 K by cooling with liquid nitrogen and resistive heating. The crystal was cleaned by 30

DOI: 10.1021/acs.jpcc.9b10358
J. Phys. Chem. C 2020, 124, 799−804

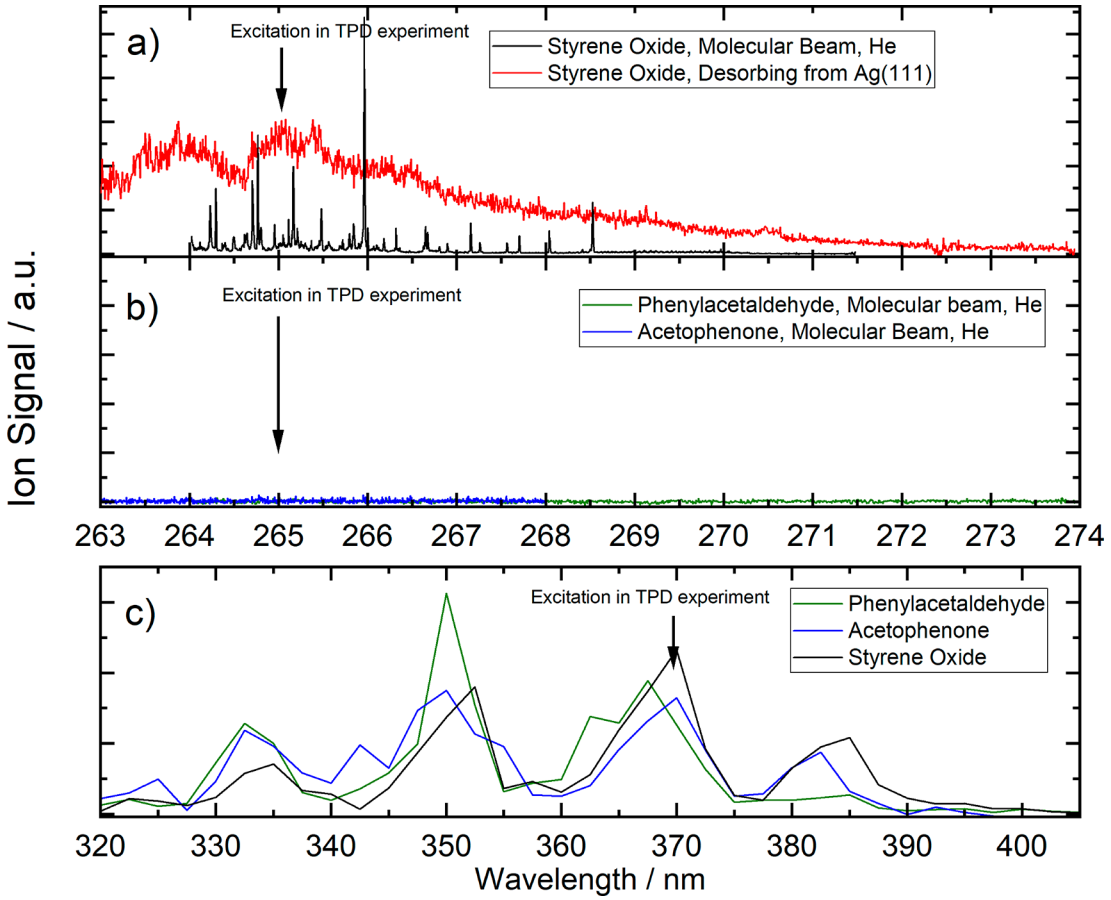

Figure 2. REMPI spectra of styrene oxide, phenylacetaldehyde, and acetophenone. (a) The black line shows the 1 + 1 REMPI spectrum of styrene oxide in the molecular beam when seeded in He and ionized with a high-resolution nanosecond dye laser. Because of the cooling in the molecular beam expansion, we resolve vibrational lines in the spectrum. The red line shows the spectrum for molecules desorbing from a Ag(111) crystal at 423 K. Because of excitation of internal degrees of freedom, the spectrum is significantly broader. (b) 1 + 1 REMPI spectrum for phenylacetaldehyde and acetophenone under the same conditions as in (a) in the molecular beam. No signal is observed. (c) 2 + 1 REMPI spectrum of styrene oxide, phenylacetaldehyde, and acetophenone when ionizing in the molecular beam with a broadband femtosecond laser. No significant difference is observed between the incident beams and desorbing molecules. The arrows indicate the frequencies to which the lasers have been tuned for REMPI-assisted TPD experiments. All spectra were recorded at the parent ion mass of 120 amu.

min Ar-ion sputtering with 10 μA surface ion current (Staib Instruments, IG-5-C) followed by 20 min surface annealing to 820 K. The cleanliness of the crystal was probed with Auger electron spectroscopy (Staib Instruments, ESA-150). We did not detect any impurities after cleaning. Desorbing molecules are resonantly ionized by the pulsed lasers described above and coupled into a ToF mass spectrometer with a 20 cm flight distance and a mass resolving power $m/\Delta m$ (fwhm) of 30. We tune the lasers to the fixed frequencies of the strong resonances at 265 and 370 nm for the 1 + 1 and 2 + 1 REMPI processes, respectively. Each laser shot creates a ToF mass spectrum which is recorded while the surface temperature is ramped linearly. Temperature control and data acquisition are achieved by a home-built Labview program. For TPD scans we heat he sample linearly at 2 K/s. For dosing we use argon (1 bar backing pressure) as seeding gas, which results in an incident molecular beam with translational energy of 250 meV. While dosing we keep the surface temperature at 200 K, which is higher than the multilayer desorption temperature which we observe at 190 K.

RESULTS AND DISCUSSION

Figure 2 shows REMPI spectra of styrene oxide, acetophenone, and phenylacetaldehyde. Panels a and b show the 1 + 1 REMPI spectra obtained by ionizing with a nanosecond laser, and panel c shows the femtosecond laser 2 + 1 REMPI spectrum. For styrene oxide we clearly resolve vibrational features in the 1 + 1 REMPI spectrum in the molecular beam due to rotational and vibrational cooling in the supersonic molecular beam expansion (see the black spectrum in panel a). The REMPI spectrum of desorbing molecules from the heated Ag(111) surface is drastically broadened as internal degrees of freedom equilibrate with the surface temperature (see the red spectrum). Using the same settings, we neither observe photoionization of acetophenone nor of phenylacetaldehyde (see panel b). In contrast, the REMPI signal is observed in the molecular beam for all three molecules when ionizing in a 2 + 1 REMPI process using femtosecond laser pulses (see panel c). The spectra look similar for all three molecules exhibiting maxima at 384, 370, 350, and 334 nm. We observe the same spectra when ionizing desorbing molecules. Here, in contrast to the nanosecond 1 + 1 REMPI spectrum, the broadening is negligible. All spectra have been recorded at the parent ion mass of 120 amu. The absence of ion signal (parent ion and

DOI: 10.1021/acs.jpcc.9b10358
J. Phys. C 2020, 124, 799−804

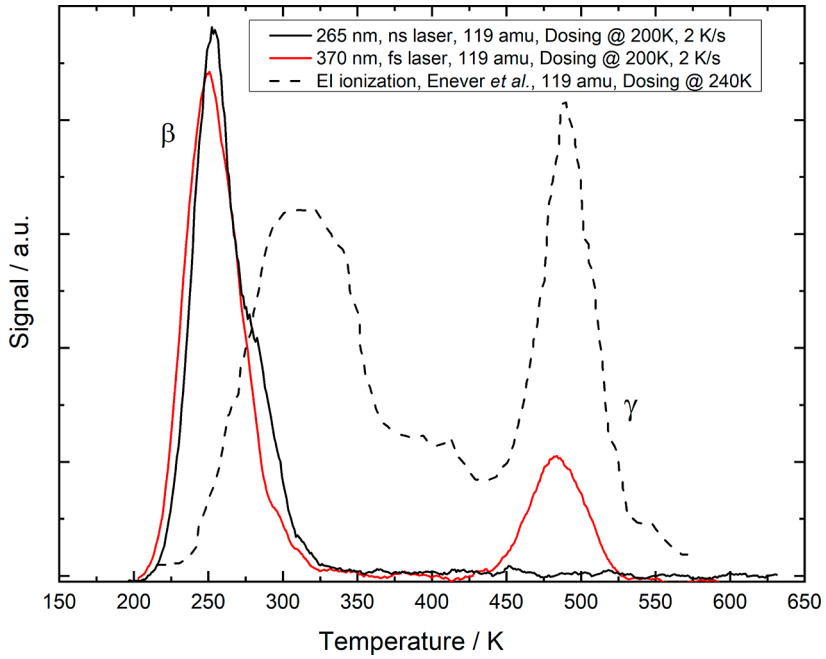

Figure 3. TPD curves for styrene oxide adsorbed on Ag(111) recorded at m/z = 119 amu. One monolayer of styrene oxide was adsorbed at a temperature above the multilayer desorption temperature. The red solid line shows the spectrum after ionizing with a femtosecond laser, the black solid line shows the spectrum after ionizing with a nanosecond laser, and the black dashed line shows the curve after electron impact ionization.[16]

fragments) when exciting phenylacetaldehyde and acetophenone with the nanosecond laser pulse is consistent with the photophysics of carbonyl molecules, which are known to undergo rapid photodissociation when excited with near-UV light.[25,26] For acetaldehyde several distinct product channels are energetically accessible following excitation to S_1, including dissociation on the electronic ground state S_0 after internal conversion (IC) and dissociation on the first excited triplet state T_1 after intersystem crossing (ISC). At higher excitation energies, photodissociation on the T_1 surface dominates, and the rate k_{ISC} of the $S_1 \rightarrow T_1$ ISC is the rate-limiting step for photodissociation. For 266 nm, k_{ISC} is 4.2×10^9 s^{-1}, corresponding to a sub-nanosecond lifetime.[25] Hence, at REMPI wavelengths around 266 nm, photodissociation is faster than multiphoton ionization on a nanosecond time scale. Assuming similar photodissociation rates for phenylacetaldehyde/acetophenone and acetaldehyde, we do not expect to detect an ion signal when exciting with a 265 nm photon produced by a nanosecond laser. In contrast, when multiphoton ionization is performed on a femtosecond time scale, ionization is faster than dissociation. Hence, femtosecond laser 2 + 1 REMPI is detected for all three molecules.

For REMPI-TPD experiments we tune the laser wavelength to 265 or 370 nm and record TPD spectra employing the nanosecond or the femtosecond laser system as photoionization source, respectively (see arrows in Figure 2). Figure 3 shows corresponding temperature-programmed desorption curves for styrene oxide adsorbed on Ag(111). The black line shows the TPD spectrum by using photoionization with nanosecond laser 1 + 1 REMPI, and the red line shows the TPD spectrum by using photoionization with femtosecond laser 2 + 1 REMPI. For comparison, the dashed line shows the curve recorded by Enerver et al. using electron impact ionization after dosing the surface with an unskimmed effusive beam source. For all three curves, the ion mass at 119 amu is recorded and the coverage is 1 ML. Both studies observe a distinct peak at a temperature between 200 and 350 K (β peak) and a peak at a temperature around 485 K (γ peak). However, differences are clearly visible.

First, in the here presented work the signal drops to zero between the two peaks whereas in the spectrum obtained by Enever et al. the peaks are less resolved. This observation may be caused by the different dosing and detection methods employed in the two studies. When dosing with a skimmed, supersonic molecular beam, only a small fraction of the surface is covered, corresponding to the molecular beam diameter of 1.5 mm. The beam is directed onto the surface, and the dosing of other parts of the sample holder is avoided. In addition, desorbing molecules are ionized by a tight laser focus ca. 20 mm in front of the surface. Hence, desorbing molecules are immediately detected after desorption avoiding background signal due to sticking to the vacuum chamber's walls.

The second difference between the study of Enever et al. and the measurements presented here is the position of the low-temperature peak. The peak presented in this study is shifted by 60 K to lower temperatures. Enever et al. dosed the surface at 240 K while we dosed at 200 K. Most likely the low-temperature peak shown in the study of Enever et al. is hence not complete as dosing was not performed below the lowest desorption temperature of the β peak. This also explains the different amplitude ratio between the γ and β peaks.

However, the most important observation presented in Figure 3 concerns the spectra recorded with different laser pulse duration in the current work. When photoionizing with a nanosecond pulse, the γ peak disappears. As the β peak is not affected by the laser pulse duration, this is strong indication that the γ and β peaks do not correspond to the desorption of the same molecule. Because only styrene oxide is ionized by nanosecond 1 + 1 REMPI (see Figure 2), the β peak is assigned to styrene oxide. However, the γ peak, which is visible only when ionizing with femtosecond laser pulses, must be produced by the desorption of either phenylacetaldehyde or

DOI: 10.1021/acs.jpcc.9b10358
J. Phys. Chem. C 2020, 124, 799−804

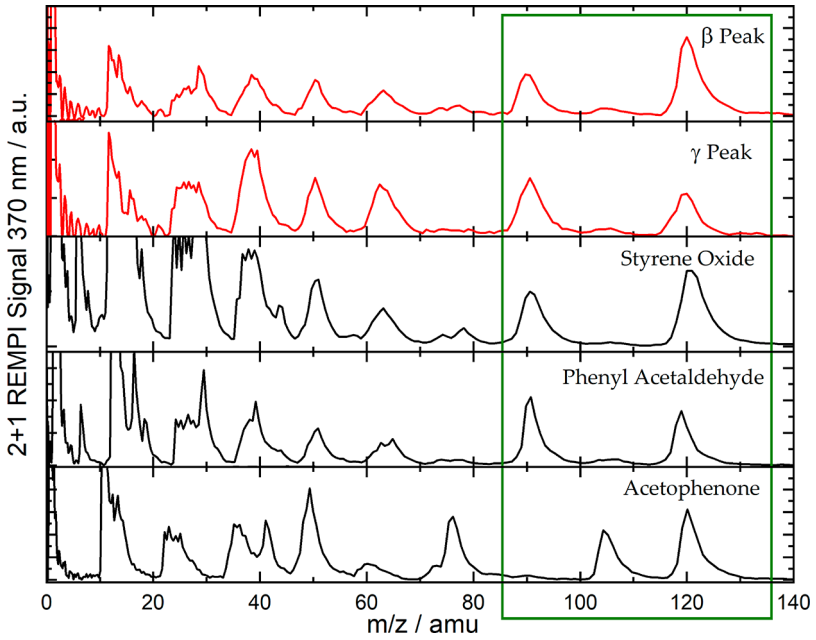

Figure 4. Mass spectra recorded at the β and γ peaks and reference mass spectra of styrene oxide and structural isomers. The ratio between the peaks at 119 and 91 amu is a strong indication that the desorption product at the γ peak is phenylacetaldehyde and the desorption product of the β peak is styrene oxide. The green rectangle indicates the region of the spectrum that was used to identify the desorbates in the β and γ peaks.

acetophenone. Both styrene oxide structural isomers are photoionized by using femtosecond 2 + 1 REMPI (see Figure 2) and are conceivable reaction products[10,11] (see Scheme 1). The reader should keep in mind that all TPD curves are recorded at the ion mass of 119 amu. Comparing the photofragmentation pattern of the γ peak with photofragmentation patterns of acetophenone and phenylacetaldehyde, we can exclude acetophenone as reaction product (see Figure 4), which shows mass spectra of the β and γ peaks as well as reference spectra for styrene oxide, phenylacetaldehyde, and acetophenone. Reference spectra were recorded by expanding the corresponding molecules in the supersonic expansion and ionizing the incident molecular beam with the femtosecond laser. The fragmentation patterns strongly suggest that phenylacetaldehyde is the molecule desorbing at high temperatures (γ peak).

These results differ from the results presented in the work of Enever et al. In contrast to our observations, they detect both isomers—phenylacetaldehyde and styrene oxide—at a desorption temperature of 485 K (γ peak). We identify two possible differences in the experimental setup that could explain the inconsistent observations.

The first difference is related to the dosing procedure. While Enever et al. dosed the surface with an unskimmed effusive beam originating from a short, stainless steel needle without a carrier gas, we employed a pulsed supersonic molecular beam source with Ar as seeding gas for dosing. Hence, styrene oxide hits the surface with an average translational energy of 250 meV in the supersonic beam, whereas the average translational energy in the effusive beam source at room temperature is probably around 30 meV. However, it is unlikely that the incidence energy in the 30−250 meV regime affects the chemisorption pathway. We confirmed this assumption by reducing the incident translational energy to 100 meV by using Xe carrier gas. Changing the dosing conditions had no detectable effect on the surface species.

The second difference concerns the ionization procedure. While molecules in this study were photoionized by using REMPI, Enever et al. employed electron impact ionization. REMPI enables a more accurate assignment of the desorbing species than it is possible for EI ionization. With EI ionization, similar fragmentation patterns of styrene oxide and phenylacetaldehyde make a clear assignment to one particular molecule more difficult. The here presented data are in agreement with the mechanism proposed by Zhou et al. for styrene oxidation:[10,11] at cold temperatures around 200 K, the oxametallacycle forms and is a stable reaction intermediate on Ag(111). When the surface is heated to temperatures around 280 K, a fraction of the oxametallacycle reacts to styrene oxide, which desorbs. The other fraction reacts after dehydrogenation to a combustion intermediate, which resembles phenylacetaldehyde (see Figure 1 in ref 11). On an oxidized surface, several reaction pathways for the combustion intermediate exist, leading to a variety of different reaction products. On a nonoxidized silver surface like we use in this study, there are no oxygen atoms at the surfaces and most pathways are unfeasible. However, back-reaction to phenylacetaldehyde and subsequent desorption is a conceivable mechanism, which is consistent with the here presented data.

CONCLUSIONS

We have used REMPI-ToF-MS-assisted temperature-programmed desorption measurements to study the reactive adsorption of styrene oxide on Ag(111). Styrene oxide undergoes ring-opening when it adsorbs on Ag(111) at 200 K. When the surface is heated, several reaction pathways are possible. Among others, ring closure followed by desorption of styrene oxide or H rearrangement and desorption of acetophenone or phenylacetaldehyde might occur. Using REMPI, we can clearly assign peaks in the TPD spectrum to styrene oxide desorbing around 250 K and to phenylacetaldehyde desorbing at 485 K. This work demonstrates how the combination of laser spectroscopy with surface

DOI: 10.1021/acs.jpcc.9b10358
J. Phys. Chem. C 2020, 124, 799−804

science techniques can provide valuable information about surface-adsorbed species and reactions at surfaces.

AUTHOR INFORMATION

Corresponding Author

*E-mail: tschaef4@gwdg.de.

ORCID

Tim Schäfer: 0000-0001-9468-0470

Notes

The authors declare no competing financial interest.

ACKNOWLEDGMENTS

We gratefully acknowledge financial support by the Deutsche Forschungsgemeinschaft under Grant SCHA 1946/2-1, G. Barratt Park for his critical reading of the manuscript, and Alec M. Wodtke for support and feedback.

REFERENCES

(1) Serafin, J. G.; Liu, A. C.; Seyedmonir, S. R. Surface Science and the Silver-catalyzed Epoxidation of Ethylene: an industrial Perspective. *J. Mol. Catal. A: Chem.* **1998**, *131*, 157−168.

(2) Huang, W.; Sun, G.; Cao, T. Surface Chemistry of Group IB Metals and related Oxides. *Chem. Soc. Rev.* **2017**, *46*, 1977−2000.

(3) Liu, X.; Madix, R. J.; Friend, C. M. Unraveling Molecular Transformations on Surfaces: a critical Comparison of Oxidation Reactions on Coinage Metals. *Chem. Soc. Rev.* **2008**, *37*, 2243−2261.

(4) Linic, S.; Barteau, M. A. Formation of a Stable Surface Oxametallacycle that produces Ethylene Oxide. *J. Am. Chem. Soc.* **2002**, *124*, 310−317.

(5) Medlin, J. W.; Monnier, J. R.; Barteau, M. A. Deuterium kinetic Isotope Effects in Butadiene Epoxidation over unpromoted and Cs-promoted Silver Catalysts. *J. Catal.* **2001**, *204*, 71−76.

(6) Lukaski, A. C.; Barteau, M. A. Investigation of Ethylene Oxide on clean and Oxygen-covered Ag(110) Surfaces. *Catal. Lett.* **2009**, *128*, 9−17.

(7) Linic, S.; Barteau, M. A. Construction of a Reaction Coordinate and a microkinetic Model for Ethylene Epoxidation on Silver from DFT Calculations and Surface Science Experiments. *J. Catal.* **2003**, *214*, 200−212.

(8) Christopher, P.; Linic, S. Engineering Selectivity in Heterogeneous Catalysis: Ag Nanowires as selective Ethylene Epoxidation Catalysts. *J. Am. Chem. Soc.* **2008**, *130*, 11264−11265.

(9) Liu, X.; Klust, A.; Madix, R. J.; Friend, C. M. Structure Sensitivity in the partial Oxidation of Styrene, Styrene Oxide, and Phenylacetaldehyde on Silver Single Crystals. *J. Phys. Chem. C* **2007**, *111*, 3675−3679.

(10) Zhou, L.; Madix, R. J. Oxidation of Styrene and Phenylacetaldehyde on Ag(111): Evidence for Transformation of Surface Oxametallacycle. *J. Phys. Chem. C* **2008**, *112*, 4725−4734.

(11) Zhou, L.; Madix, R. J. Strong Structure Sensitivity in the partial Oxidation of Styrene on Silver single Crystals. *Surf. Sci.* **2009**, *603*, 1751−1755.

(12) Zhou, L.; Gorin, C. F.; Madix, R. J. Cesium Promotion in Styrene Epoxidation on Silver Catalysts. *J. Am. Chem. Soc.* **2010**, *132*, 434−435.

(13) Carbonio, E. A.; Rocha, T. C. R.; Klyushin, A. Y.; Píš, I.; Magnano, E.; Nappini, S.; Piccinin, S.; Knop-Gericke, A.; Schlögl, R.; Jones, T. E. Are Multiple Oxygen Species selective in Ethylene Epoxidation on Silver? *Chemical Science* **2018**, *9*, 990−998.

(14) Klust, A.; Madix, R. J. Selectivity Limitations in the Heterogeneous Epoxidation of Olefins: Branching Reactions of the Oxametallacycle Intermediate in the Partial Oxidation of Styrene. *J. Am. Chem. Soc.* **2006**, *128*, 1034−1035.

(15) Wang, C.; Wei, Z.-Z.; Lü, Y.-K.; Xing, B.; Wang, G.-C. Theoretical Investigation of Structure-Sensitivity of Styrene Epoxidation on Ag(111) and Ag(110) Surfaces. *Acta Phys.-Chim. Sin.* **2013**, *29*.

(16) Enever, M.; Linic, S.; Uffalussy, K.; Vohs, J. M.; Barteau, M. A. Synthesis, Structure, and Reactions of Stable Oxametallacycles from Styrene Oxide on Ag(111). *J. Phys. Chem. B* **2005**, *109*, 2227−2233.

(17) Sugimoto, T.; Fukutani, K. Effects of Rotational-Symmetry Breaking on Physisorption of Ortho- and Para-H_2 on Ag(111). *Phys. Rev. Lett.* **2014**, *112*, 146101.

(18) Winbauer, A.; Kollmannsberger, S. L.; Walenta, C. A.; Schreiber, P.; Kiermaier, J.; Tschurl, M.; Heiz, U. Isomer-Selective Detection of aromatic Molecules in Temperature-Programmed Desorption for Model Catalysis. *Anal. Chem.* **2016**, *88*, 5392−5397.

(19) Park, G. B.; Krüger, B. C.; Meyer, S.; Schwarzer, D.; Schäfer, T. The ν_6 Fundamental Frequency of the $\tilde{A}$ State of Formaldehyde and Coriolis Perturbations in the $3\nu_4$ Level. *J. Chem. Phys.* **2016**, *144*, 194308.

(20) Krüger, B. C.; Schäfer, T.; Wodtke, A. M.; Park, G. B. Quantum-state Resolved Lifetime of Triplet ($\tilde{a}^3A_2$) Formaldehyde. *J. Mol. Spectrosc.* **2019**, *362*, 61−68.

(21) Harding, D. J.; Neugebohren, J.; Hahn, H.; Auerbach, D. J.; Kitsopoulos, T. N.; Wodtke, A. M. Ion and Velocity Map Imaging for Surface Dynamics and Kinetics. *J. Chem. Phys.* **2017**, *147*, 013939.

(22) Akiyama, I.; Li, K. C.; LeBreton, P. R.; Fu, P. P.; Harvey, R. G. Ultraviolet Photoelectron Studies of polycyclic aromatic Hydrocarbons. The Ground-state electronic Structure of Aryloxiranes and Metabolites of Benzo[a]pyrene. *J. Phys. Chem.* **1979**, *83*, 2997−3003.

(23) Distefano, G.; Granozzi, G.; Bertoncello, R.; Olivato, P. R.; Guerrero, S. A. Hyperconjugative Interactions in Halogen-substituted Carbonyls: Ultraviolet Photoelectron Spectroscopy of ω-halogenoacetophenones. *J. Chem. Soc., Perkin Trans. 2* **1987**, *2*, 1459−1463.

(24) Rabalais, J. W.; Colton, R. J. Electronic Interaction between the Phenyl Group and its unsaturated Substituents. *J. Electron Spectrosc. Relat. Phenom.* **1972**, *1*, 83−99.

(25) Toulson, B. W.; Kapnas, K. M.; Fishman, D. A.; Murray, C. Competing Pathways in the near-UV Photochemistry of Acetaldehyde. *Phys. Chem. Chem. Phys.* **2017**, *19*, 14276−14288.

(26) Harrison, A. W.; Kable, S. H. Photodissociation Dynamics of Propanal and Isobutanal: The Norrish Type I Pathway. *J. Chem. Phys.* **2018**, *148*, 164308.

DOI: 10.1021/acs.jpcc.9b10358
J. Phys. Chem. C 2020, 124, 799−804